Laidlaw Undergraduate Leadership and Research Programme 2025

Investigating Abdominal Metamorphosis in Dipteran Insects

Alexandra Ermolenko

Supervisor: Dr. Marcus Bischoff

School of Biology, University of St Andrews

Table of contents

Summary

Research into the metamorphosis of the adult abdominal epidermis in the Brachyceran fly *Drosophila melanogaster* has significantly contributed to the current understanding of the cellular and molecular mechanisms controlling adult development in flies. During this process, adult precursor cells (histoblasts) replace the larval epithelial cells (LECs) forming the adult skin. However, little to no research has been done on characterising metamorphosis in the lower suborder of flies of the Diptera order, the Nematocerans. The report provides a foundation for studying metamorphosis of the adult abdominal epithelium in the Nematocerans through a description of the types of epithelial cells present in the larvae and pupae of a mosquito (*Anopheles stephensi*) and a fungus gnat (family Sciaridae) across several developmental stages. Using Hoechst staining and confocal microscopy, I have captured images of the nuclei of epithelial cells in different positions along the abdomen of the specimens. In the mosquito epithelium, I found no evidence of the presence of progenitor cells and LECs show a homogenous distribution throughout development. LEC size varies through larval and pupal stages and cell divisions were observed. In the fungus gnat, in between regions of large nuclei, regions with smaller nuclei were present, suggesting that there may be adult precursor cells positioned among the LECs. These observations suggest that a mode of metamorphosis that employs adult precursor cells may be found in the Bibionomorpha infraorder, but not the Culicomorpha.

1. Introduction

Insects are one of the most well-known animals to undergo metamorphosis. The term ‘metamorphosis’ encompasses the complete biological transformation of the organism from the immature form to the adult form (Truman, 2019). The lifecycle trajectory for the insect orders that undergo full metamorphosis follows four distinct stages: egg, larva, pupa, and the adult. The larval stage often has several instars, with the last instar pupating. Then, the larval structures are replaced by adult structures in the new pupa, with the adult later eclosing from the pupal cuticle (Truman, 2019).

The evolution of metamorphosis is an interesting phenomenon, as complete metamorphosis was not present in the ancestral insect species, with some modern-day insect species still undergoing direct development (ametabolous metamorphosis) (Truman and Riddiford, 1999). Complete metamorphosis (also known as holometabolous metamorphosis),

where the larva completely remodels into the adult, contributed to the diversity of developmental mechanisms and insect forms. From an evolutionary perspective, the advantage offered by the transitions between the different body plans of the larva and adult is the potential for a higher survival rate, as each stage can utilize different resources in various surroundings (Truman and Riddiford, 1999).

Little is known about how the cellular mechanisms underlying metamorphosis have evolved. The most popular model used for investigating cellular rearrangements during metamorphosis is the Brachyceran fruit fly, *Drosophila melanogaster*. During Drosophila metamorphosis, many of the adult structures, e.g. wings, legs and eyes, arise from imaginal discs that are epithelial sacs that grow during larval stages and form the adult structures during metamorphosis (Madhavan and Madhavan, 1980; Truman, 2019). Abdominal metamorphosis, on the other hand, is characterized by cell replacement, whereby the polyploid larval epithelial cells (LECs) are replaced by diploid progenitor cells (histoblasts) (Fig. 1a; Roseland and Scheiderman, 1979; Madhavan and Madhavan, 1980). Histoblasts are created during embryogenesis, arranged in small nests and dormant in the larval stages (Truman, 2019). The replacement process begins after pupariation when the histoblasts begin to divide (Roseland and Scheiderman, 1979; Madhavan and Madhavan, 1980). Then, the histoblasts replacing the LECs that undergo programmed cell death (Ninov *et al.*, 2007; Bischoff and Cseresnyés, 2009).

Such a cell replacement process has only been described in Brachyceran diptera (Fig. 2) (including *Calliphora erythrocephala*, *Sarcophaga agryostoma,* and the family Sepsidae) (Melicher *et al.*, 2018; Pearson, 1977; Smith and French, 1991)). In other insects, the adult abdominal epidermis arises by LEC transdifferentiation, where the LECs survive metamorphosis and become adult cells (Fig. 1b; Truman, 2019). Two examples of such insects are *Galleria melonella* (Kumaran, 1978) and *Hyalophora cecropia* (Sedlak and Gilbert, 1976).

It is unclear how the replacement mode of abdominal metamorphosis has evolved in the Diptera. It could have evolved at the basis of the Diptera (so all Diptera display cell displacement) or in one or more lineages within the Diptera. As cell replacement has been described in Brachyceran species, I ask here which mode of abdominal metamorphosis can be found in Nematoceran flies (replacement vs. reprogramming).

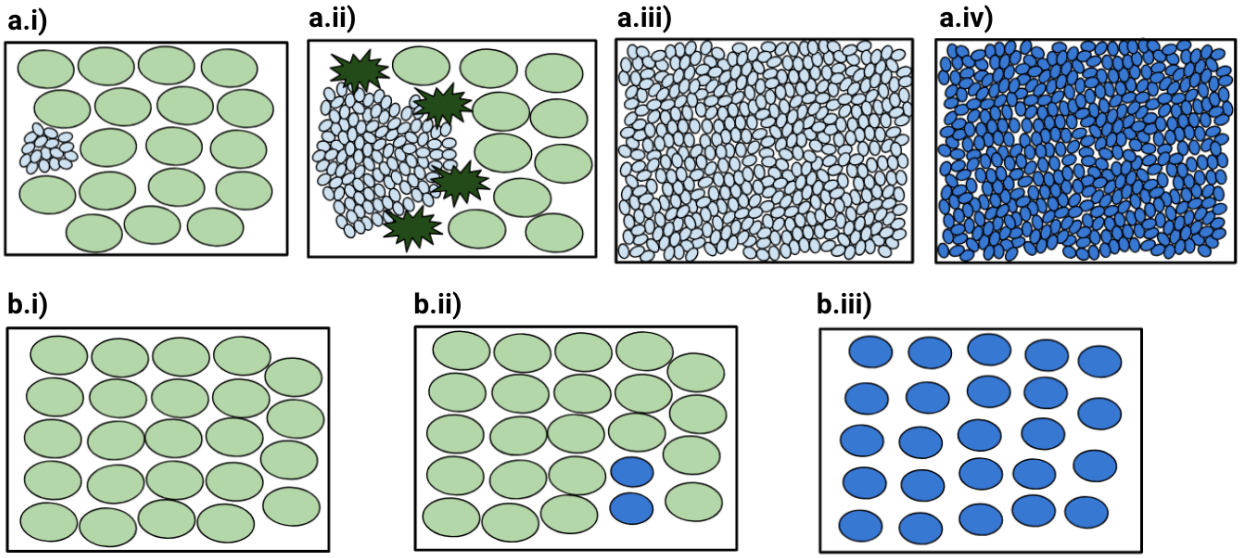

Fig. 1: Two modes of abdominal metamorphosis. Blue, adult cells, green larval cells. (a) Scheme demonstrating the replacement mode of abdominal metamorphosis where the adult progenitor cells (histoblasts) are present as a small, lateral nest (a.i) which then begins to proliferate and expand across the abdominal epithelium (a.ii), while the larger larval epithelial cells (LECs) undergo apoptosis, which is represented by the irregular shapes. The histoblasts continue to proliferate until there are no more LECs (a.iii), before differentiating into adult cells that compose the adult abdominal epidermis (a.iv). (b) Scheme showing the de-differentiation and proliferation of LECs (b.ii and b.iii) without precursor cells (b.ii).

To this end, I investigated a species belonging to the infraorder Culicomorpha, the mosquito *Anopheles stephensi*, and a species belonging to the infraorder Bibionomorpha, an unidentified fungus gnat species (Fig. 2).

To investigate abdominal metamorphosis in these Nematocerans, I used Hoechst 34580 to label the nuclei of larval and pupal cells, allowing me to assess cell numbers and nuclear size using confocal microscopy. The results suggest that in *A. stephensi* there are only LECs present without evidence for adult precursor cells and cell replacement. This suggests that *A. stephensi* employs a reprogramming mode of metamorphosis. In the fungus gnat, on the other hand, I found potential evidence for groups of adult precursor cells with small nuclei surrounded by larger LECs. These results provide initial evidence that may suggest that cell replacement has evolved in the Neodiptera.

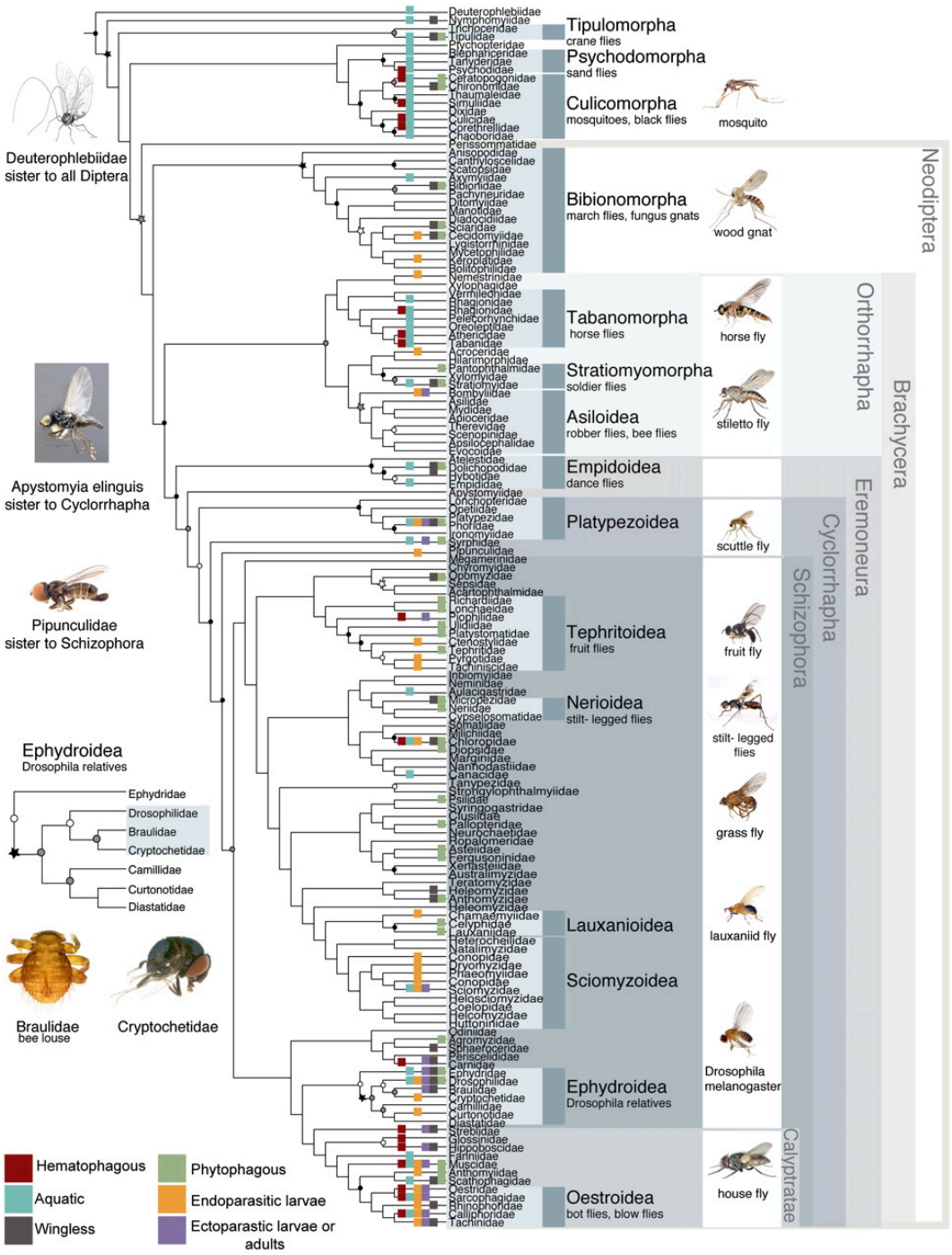

Fig. 2: A phylogenetic tree of the Diptera. The *Drosophila melanogaster* fruit fly belongs to the Brachyceran Ephydroidea superfamily, whilst the two Nematoceran Ditperan used in this report, the unidentified fungus gnat species (family: Sciaridae) and *A. stephensi* mosquito (family: Culicidae), belong to the Bibionomorpha and the Culicomorpha infraorders, respectively. Both the fruit flies and the fungus gnats are Neodipterans. The figure was taken from Wiegmann *et al*., 2011.

2. Methods and Materials

2.1 Dipteran stocks

2.1.1 *A. stephensi* culture and collection

Larvae of *A. stephensi* were provided by the Reece lab (University of Edinburgh) and grown in 2 plastic ice cream containers with water at room temperature (RT, 21ºC) exposed to natural light (approximately 17 hours of daylight and 7 hours of dark). The larvae were provided with four fish food pellets a day. The developmental stages chosen for the mosquitoes were early larval fourth instars (L4s), late L4s, 20–40-minute old pupae, and 6-hour old pupae (Figs. 3, 4). The analysed specimens were not sexed.

a) early L4 b) late L4

Fig. 3: *A. stephensi* larval fourth instars (L4) chosen for the investigation. The early L4 (a) was identified based on its size (it is larger than the earlier instars), the appearance of the orange hue in the midline, and the thorax length to head length ratio (where in the early L4 the thorax is slightly longer in diameter than the head). The late L4 (b) was identified based on the disappearance of the orange hue in the midline, the appearance of the milky white colour throughout the body, and the visibly larger thorax compared to the head. Approximately 1 hour after the image of the late L4 (b) was taken, the late L4 underwent pupation. The physiological appearance of the late L4 corresponds to 1 hour before pupation. The photos were taken using an iPhone 15 camera through the eyepiece of a light microscope.

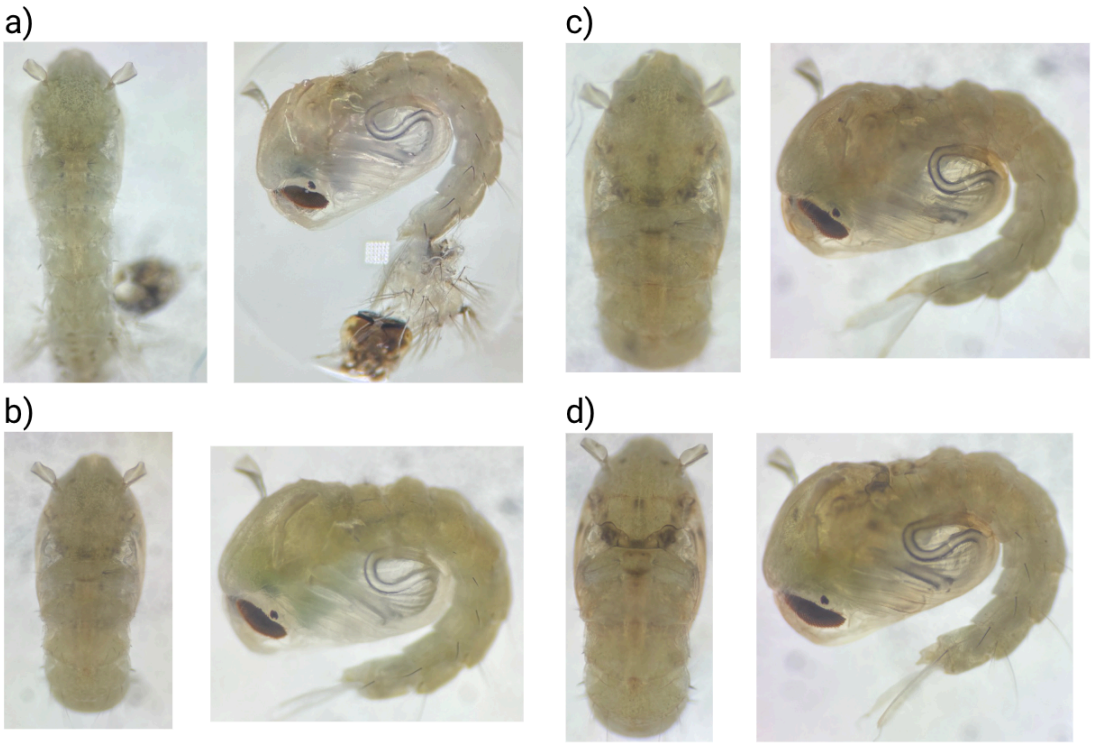

Fig. 4: *A. stephensi* pupae from a dorsal and lateral perspective at different times after pupation: 20 minutes (a), 40 minutes (b), 4 hours (c), and 6 hours (d). The photos are not to scale and were taken using an iPhone 15 camera through the eyepiece of a light microscope.

To determine the appearance of the early and the late L4s of *A. stephensi*, groups of larvae that had a similar physiological appearance were collected from the containers using a plastic pipette and put in droplets on a petri dish. The petri dish was kept under close observation and looked at under a light microscope at irregular intervals. If there was a marked difference in any of the larvae a photo was taken. The early L4 (Fig. 3a) was identified using the presence of an orange hue in the midline, a larger size compared to the other instars, and a similar width of the thorax and the head. The late L4 (Fig. 3b) could be identified due to its milky white appearance and the increased diameter of the thorax compared to the head. The pupation of the late L4 was observed under a stereomicroscope (Leica MZ10 F) equipped with a camera (AmScope MU300-HS).

The *A. stephensi* pupae were kept under close observation to time them and to be able to track their physiological appearance throughout development. The larvae that were observed to have undergone pupation in real-time and the pupae that still had the larval skin attached to the tail were transferred into petri dishes from the containers using a pipette and timed from the

time of pupation. This was repeated for each desired ‘time after pupation’ group of pupae before dissection.

2.1.2 Fungus gnat collection

Fungus gnats were collected from indoor plant pots in the write-up area of the Bischoff lab. The search for fungus gnat larvae and pupae occurred in the morning. The soil from the indoor plant pots was poured into a large plastic tray and the soil was moved around with a spatula to find the desired specimens. The fungus gnat larvae and pupae were collected using a damp paintbrush. The developmental stages chosen for the fungus gnats were early L4s, late L4s, and pupae of a variable, unknown time after pupation collectively called “late pupae”. The developmental stages chosen were defined based on morphology (Fig. 5). The analysed specimens were not sexed.

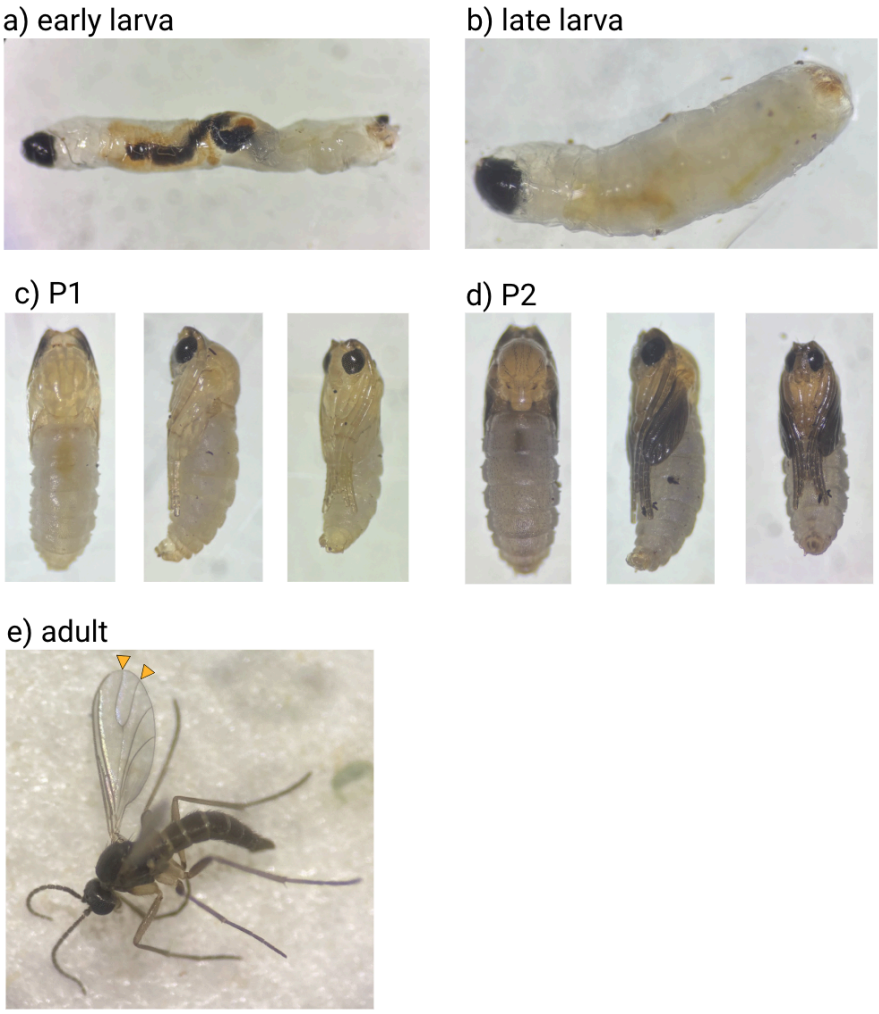

Fig. 5: Fungus gnat larvae and pupae at different stages of development chosen for the investigation. The early L4 (a) was identified based on its visible size and length compared to the other larvae found in the soil. The late L4 was a rare occurrence and was spotted based on its immobility. Since it was not possible to time the pupae, both P1 (c) and P2 (d) were classed as 'late pupae' for the purposes of this report, although P2 is pigmented and thus at a later stage than P1. The images for P1 (c) and P2 (d) depict the pupae from dorsal, lateral, and ventral perspectives, respectively. The wing venation in the adult (e) confirmed that it is a fungus gnat. The images (a-d) were taken using an iPhone 15 camera through the eyepiece of a light microscope.

2.1.3 Temporary fungus gnat culture

To attempt to establish a fungus gnat culture, adult fungus gnat adults were collected from the indoor plant pots and placed in Erlenmeyer flasks covered with cotton and filled with soil from

the respective plant pot. The wing venation in the adult confirmed that it is a fungus gnat (Kuiter, 2020). Honey was provided in a small aluminium foil bowl, to serve as a source of nutrition for the adults (Gillespie, 1986). The fungus gnats were grown at RT. The gnats survived for several weeks in the flasks and produced offspring. It was not attempted to maintain the colony when this project finished.

2.2 Sample preparation and imaging

2.2.1 Dissection

The specimens of the desired developmental stage were placed on double-sided sticky tape on a glass slide and were immediately dissected using a scalpel. The specimen sizes were not recorded. The cut axes for the larvae and pupae of the fungus gnat and *A. stephensi* are shown in Fig. 6, although it was not always possible to cut it as precisely as depicted in the figure. The latter meant that the abdominal segments used for staining and visualization were not identical.

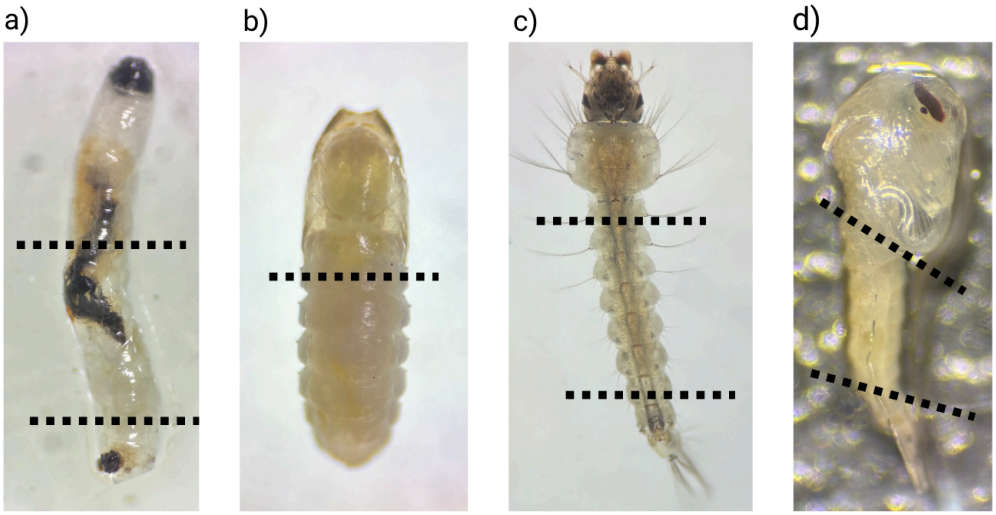

Fig. 6: Cut axes for the larvae and pupae of fungus gnats (a and b, respectively) and *A. stephensi* (c and d, respectively). The dotted lines represent the approximate cuts made with a scalpel, although it was not always possible to follow these exactly. The images were taken using an iPhone camera through the eyepiece of a light microscope.

2.2.2. *In vivo* Hoechst staining

Nuclei in living mosquito larvae were stained using the live stain Hoechst 34580 (Sigma-Aldrich). The samples were removed from the tape using a phosphate-buffered saline

(PBS) droplet and placed into 2 µg/mL Hoechst 34580 for 30 minutes. The samples were then placed into PBS for 5 minutes before being mounted on a glass slide that was sealed with Vaseline petroleum jelly.

2.2.3 Hoechst staining after fixation

The dissected samples were kept in PBS droplets until all specimens were dissected. The dissected samples were transferred to 4% paraformaldehyde (PFA) solution in a 6-well plate for 30 minutes at RT for tissue fixation. If larvae and pupae were dissected simultaneously, they were kept in separate wells to avoid mixing them up. The samples were placed in PBS for 5 minutes before being put into PBS-Tween solution (0.1 % Tween 20) for 30 minutes to permeabilize the tissue. To stain the samples, they were set in 4 µg/mL Hoechst 34580 for 40 minutes in the refrigerator at 4ºC in the darkness. After the time had elapsed, the samples were taken out and transferred to PBS for 5 minutes. Finally, the samples were carefully positioned in droplets of VectaShield antifade mounting medium on a glass slide and sealed with Vaseline petroleum jelly. All prepared glass slides were stored in the refrigerator at 4ºC. The staining of the samples was visualized on a Leica SP8 confocal microscope (Leica Microsystems, Germany) using a diode laser at 405 nm with the 20x / 0.75 objective.

2.3 Nuclear diameter measurement

The nuclei diameters in the images taken on the confocal microscope were measured using Fiji (Schindelin *et al.*, 2012). It was not possible to measure all epithelial cell nuclei in the abdominal segments; thus, a total of 14 nuclei were measured per image. The nuclei were measured by drawing a line across the nuclei to measure the diameter. The criteria for image selection included low magnification, clear visibility of nuclear outlines, inclusion of only the upper z-stacks, and the largest possible visible surface area of the abdominal region. Depending on the nuclei distribution across the image, the image was visually divided into separate areas. Then, an area would be zoomed in upon and several nuclei diameter measurements were taken of non-neighbouring cells. Afterwards, the area would be changed and a proportionate number of measurements to the previous area was made, ensuring a distributed sample size.

For fungus gnats, six images of separate specimens for each developmental stage were chosen for the purposes of nuclei measurement in subsection 3.2.2. Where there were visible

small cell populations in the abdomen (subsection 3.2.1), the measurements were taken of the larger LECs and the small cells separately.

To measure the mean nuclei diameter in the *A. stephensi* abdomen, five images were selected of five separate specimens for each developmental stage. Due to the availability of data for the dorsal side and the lack thereof for the ventral side for *A. stephensi*, the measurements for section 3.1.4 were made using the dorsal side. The latter is important to note, because there was a difference noticed between the nuclei sizes for the larval dorsal and ventral sides of *A. stephensi* (Fig. 11).

2.4 Statistics

The Shapiro-Wilk test was used to verify the normal distribution of the nuclei diameters in Tab. 1 and Tab. 3. Then, Bartlett's test was utilized to check for equal variance in the samples. The variance equal ($p>0.05$); thus, the One-Way Analysis of Variance (ANOVA) was used to test the statistical significance between the nuclei diameters of every developmental stage for *A. stephensi* and the fungus gnats. Lastly, Tukey's Honestly Significant Difference (HSD) post-hoc test was applied to the data to see where the statistical differences are. All tests were done in R (R Core Team, 2024). The rstatix package (Kassambra, 2023) was used for the Shapiro-Wilk test, Bartlett's test, One-Way ANOVA, and Tukey's HSD, and the stats package (R Core Team, 2024) was used for Bartlett's test.

3. Results

3.1 Metamorphosis of the abdominal epidermis of *A. stephensi*

3.1.1 Live imaging of the pupation of *A. stephensi*

To allow staging of the metamorphosis of *A. stephensi*, I first imaged pupation under a stereomicroscope. A distinguishing feature of a late L4 about to undergo pupation are the anterior spiracles of the pupa (called trumpets), which are present on either side of the anterior edge of the larval thorax (Fig. 7a.i) (Nishiura, 2002). The trumpets are the first to emerge from the larval cuticle during pupation (Fig. 7b.i). The pupation of *A. stephensi*, occurring over a period of approximately 7 minutes, can be likened to the removal of a helmet, where the eyes are drawn back into the emerging pupal head as the larval head is removed. The coordinated contraction and relaxation of the abdominal muscles remove the rest of the larval cuticle, with

the cuticle sometimes remaining attached to the pupa's tail for another 30 minutes post-pupation. Knowledge of the progression of pupation allowed me to time pupae for my experiments.

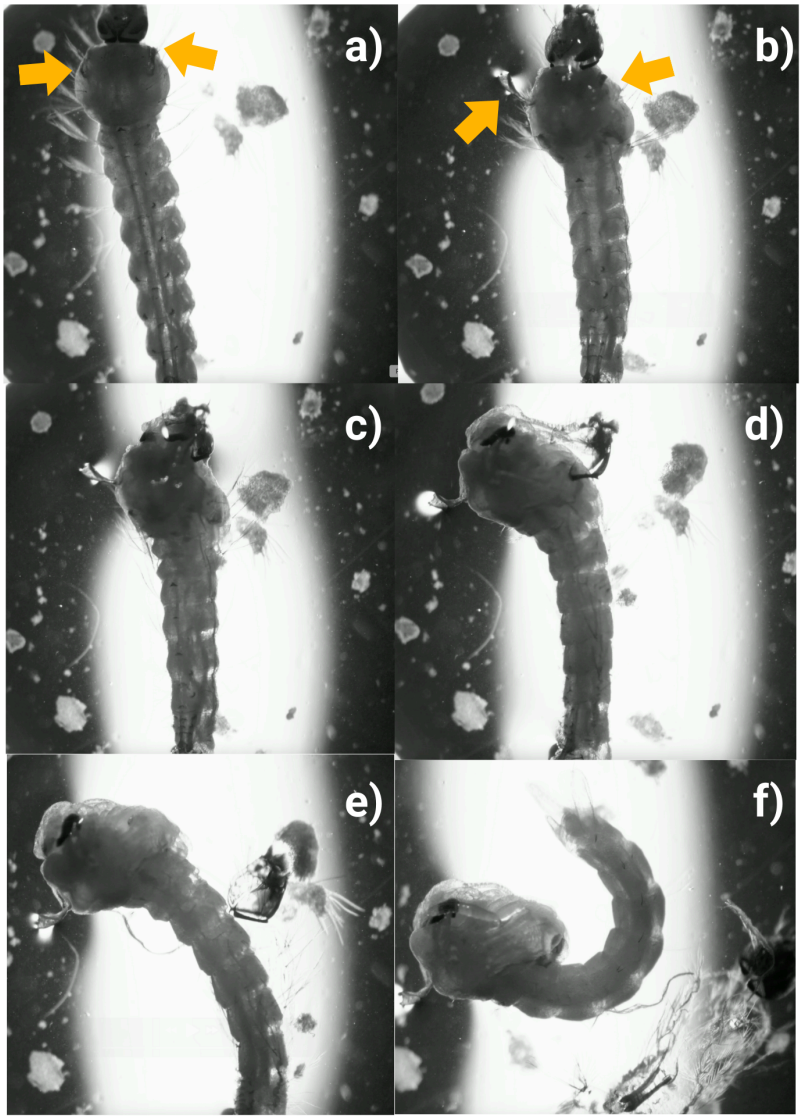

Fig. 7: Live imaging of the pupation of *A. stephensi*. It is possible to identify the two trumpets of the emerging pupa, indicated by the arrows, in (a) and (b). The larva undergoing pupation (a) twitches and the trumpets at the anterior end of the thorax are the first to emerge from the larval cuticle (b). The head of the larva comes off (c) and the head of the pupa emerges (d). Subsequently, the pupa begins to remove the larval cuticle by pulling it downwards as seen in (e). (f) shows the pupa free from the larval cuticle. The images were taken from a video covering all of the pupation.

3.1.2 Comparison of protocols used to stain the *A. stephensi* abdominal epidermis

The live staining of mosquito tissues using Hoechst 34580 resulted in a variety of background signals, which formed large, irregular clusters, in addition to the staining of the nuclei in the abdominal epidermal tissue (Fig. 8). This background signal was presumed to be caused by autofluorescent lipid vesicles and/or pigments, as fixation and permeabilization of the tissue removed the signal (Fig. 9). As the signal made distinguishing nuclei in the tissue samples of *A. stephensi* more difficult, the fixed tissues were used for the subsequent analyses.

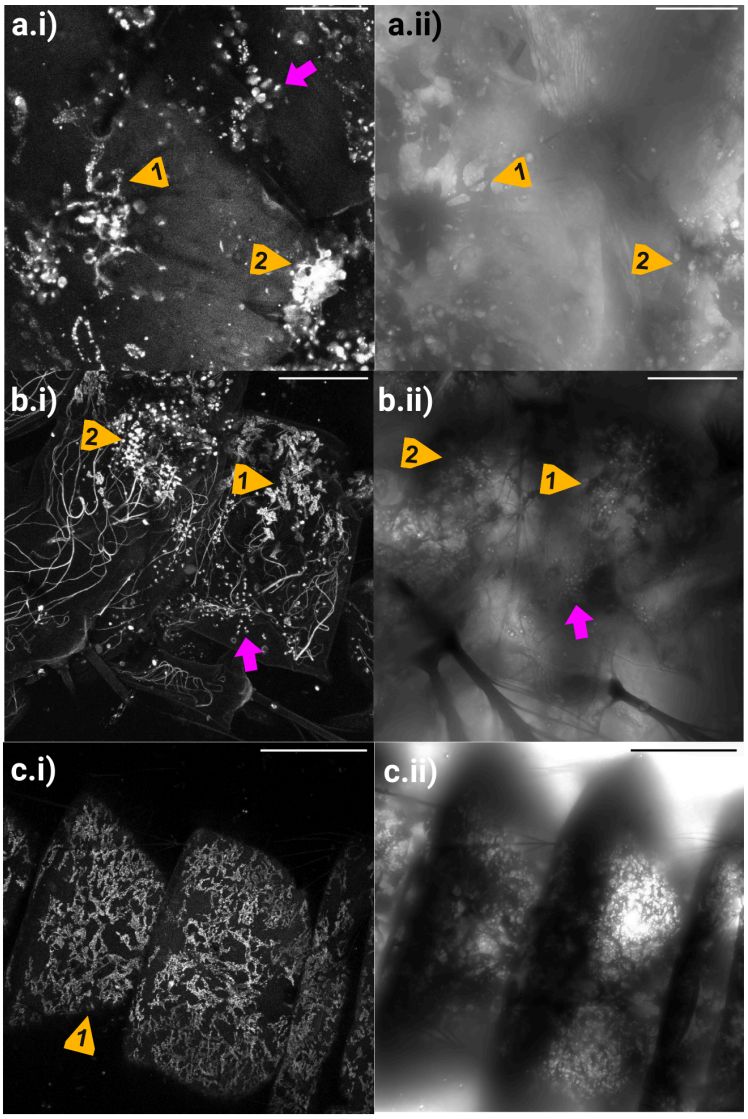

Fig. 8: The *A. stephensi* larvae and pupae tissue samples produced by the live staining protocol. (b) Mosquito larvae, (a,c) mosquito pupae. The live staining protocol tissue samples (a-c) show an autofluorescent signal, which may be pigment clusters (arrowhead 1) and lipid droplets

(arrowhead 2). The transmitted light images (a.ii, b.ii, c.ii) were included to show the clusters. The nuclei are indicated by unnumbered arrows. Scale bars, 40 μm (a), 100 μm (b), 200 μm (c).

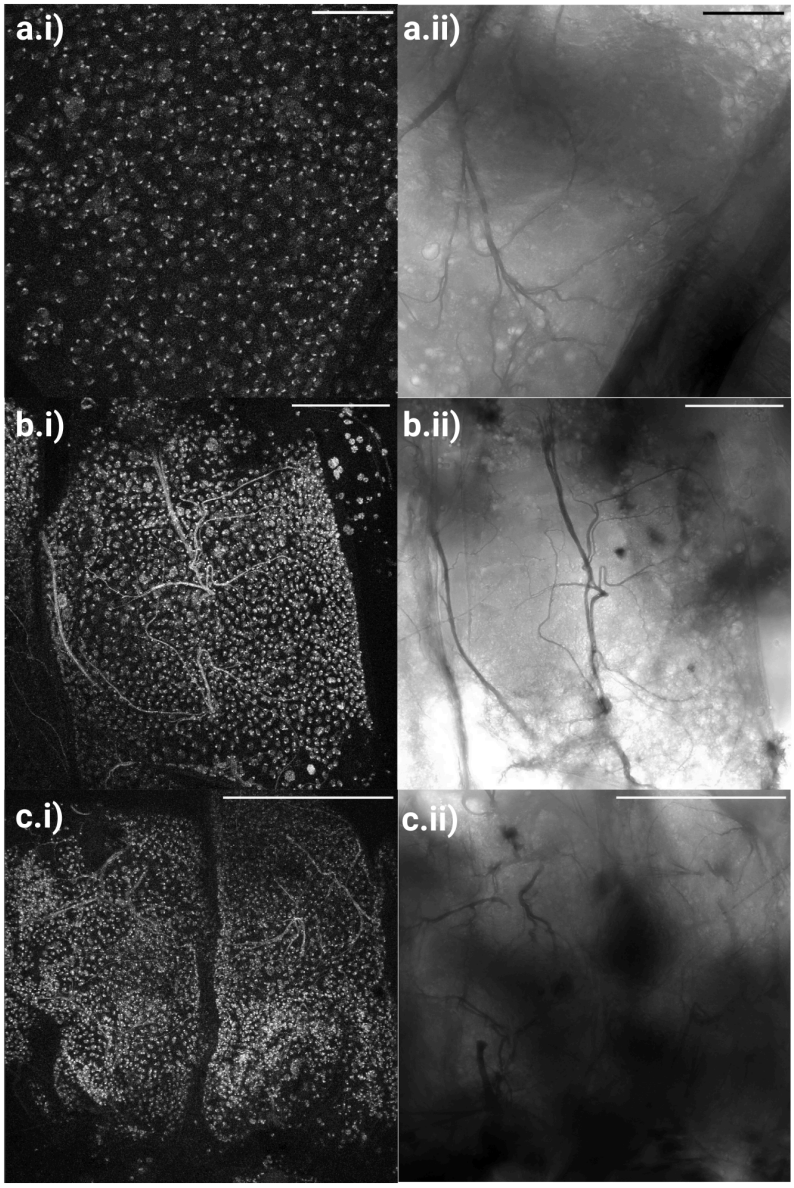

Fig. 9: The *A. stephensi* larvae and pupae tissue samples produced by the fixation protocol. fixation protocol tissue samples show little background signal. (b) Mosquito larva, (a, c) mosquito pupae. There is no background signal (a.i, b.i, c.i) and the epithelial nuclei are clearly visible across the abdominal segment. The transmitted light images (a.ii, b.ii, c.ii) were included to show that the clusters seen with the live staining protocol were removed. Scale bars, 40 μm (a), 100 μm (b), 200 μm (c).

3.1.3 Cell composition of larval and pupal abdominal epidermis in *A. stephensi*

A homogeneous cell population (Fig. 10) was observed which with respect to nuclei distribution, did not change much across all developmental stages. This was seen across 104 images taken of all 4 stages. There were no regions in the epithelium where the cells were significantly smaller.

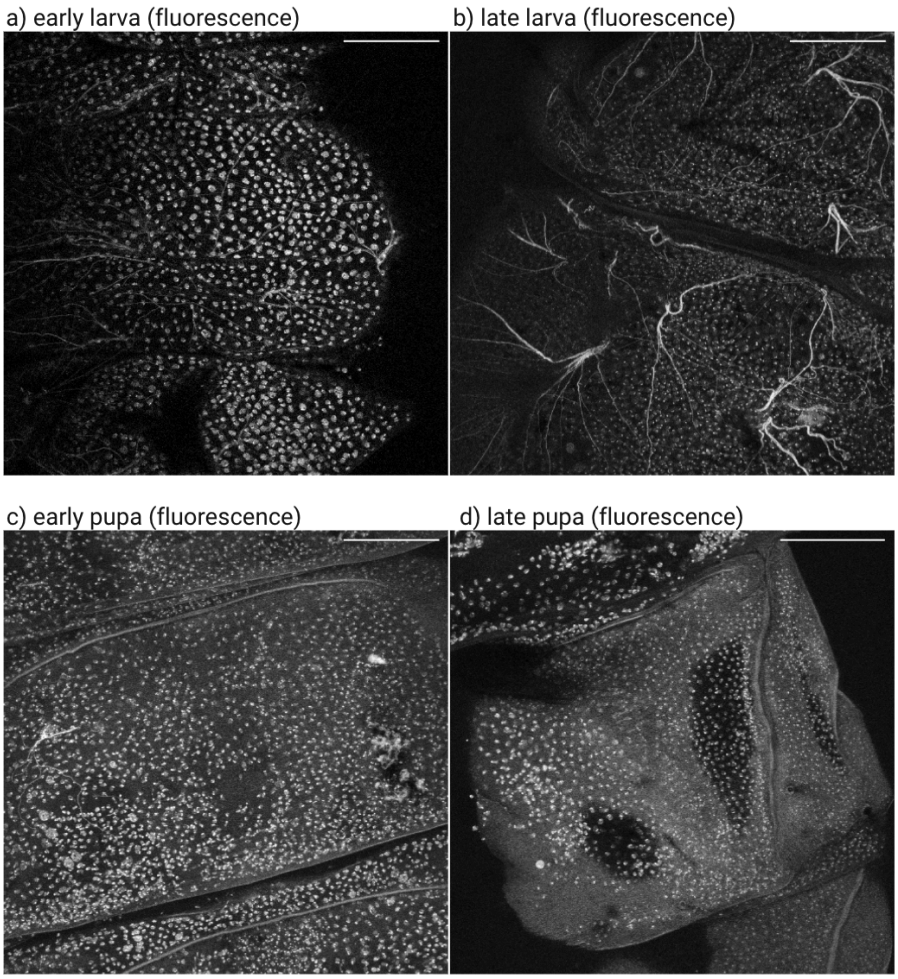

Fig. 10: The dorsal abdominal epithelium of *A. stephensi* across 4 developmental stages. The nuclei distribution remains consistently homogenous for all 4 stages. (a) early larval fourth instar, (b) late larval fourth instar, (c) shows a 20-minute old pupa, (d) 6-hour old pupa. Throughout development, the nuclei in the epidermis become smaller (nuclear diameter is 6.5 ± 1.6 μm (a), 6.3 ± 0.9 μm (b), 5.3 ± 1.3 μm in panel c, and 4.4 ± 1.5 μm in panel d). Scale bars, 100 μm.

Larval stages

The first stages that were looked at were the early and late L4s, with the dorsal side being the most predominant in the dataset. The early L4s (Fig. 10a) had relatively larger epithelial cell nuclei on the dorsal side compared to the dorsal sides of the subsequent stages. The next stage, the late L4 (Fig. 10b), tended to exhibit an occasionally smaller cell nuclei diameter on its dorsal side than the previous stage. In both stages, the dorsal and ventral sides had a homogenous distribution, although the ventral and the dorsal epithelia have different nuclei sizes. The ventral side has smaller nuclei (Fig. 11a-b). In addition, on the more lateral side of the ventral epithelia there were spiracles that had very small nuclei (2.0 ± 0.8; μm Fig. 11b.ii).

For both larval developmental stages, evidence for cell division was found (Fig. 12). The dividing cells were found to be either fully divided or undergoing cytokinesis.

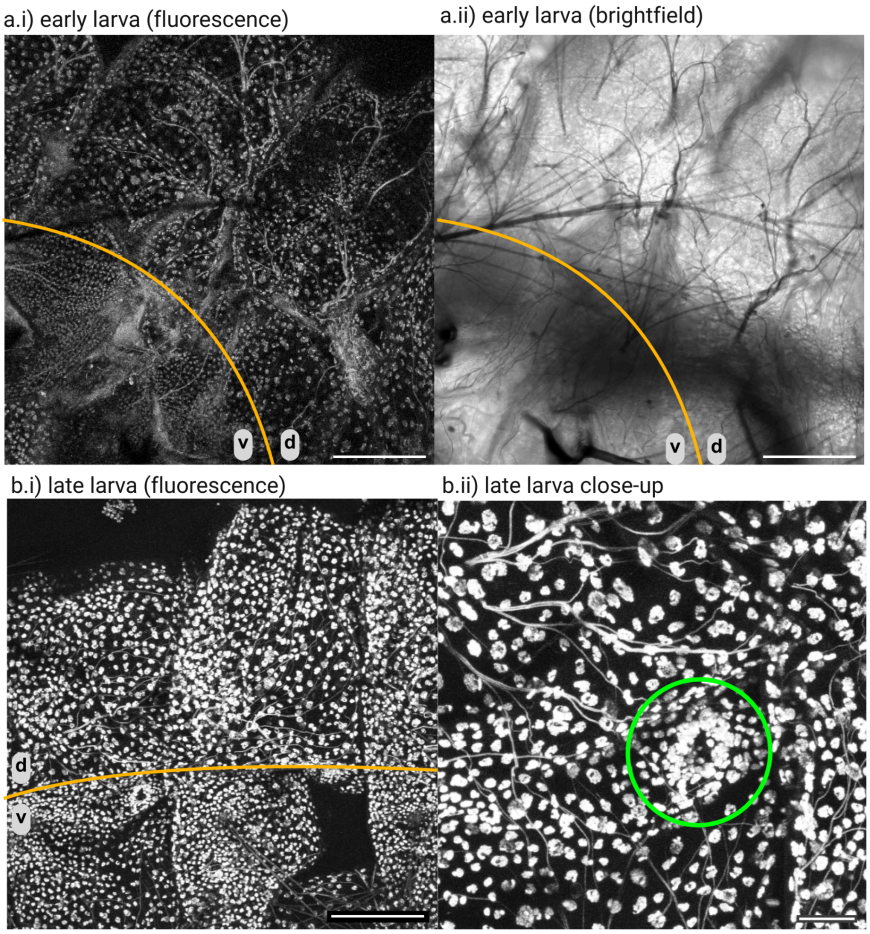

Fig. 11: The lateral perspective of the larvae abdomens of *A. stephensi*. The line across the abdominal segment shows the lateral axis dividing the dorsal (d) and ventral (v) sides. The early L4 in panels a.i and a.ii has a nuclei diameter of 3.2 ± 1.3 μm on the ventral side and 6.1 ± 1.6

μm on the dorsal side. Panel b.i features a late L4 that has a nuclei diameter of 3.9 ± 1.4 μm on the ventral side and 5.8 ± 1.5 μm on the dorsal side. The circled group of small cells (b.ii) is a spiracle. Scale bars: 100 μm (a-b.i), 20 μm (b.ii).

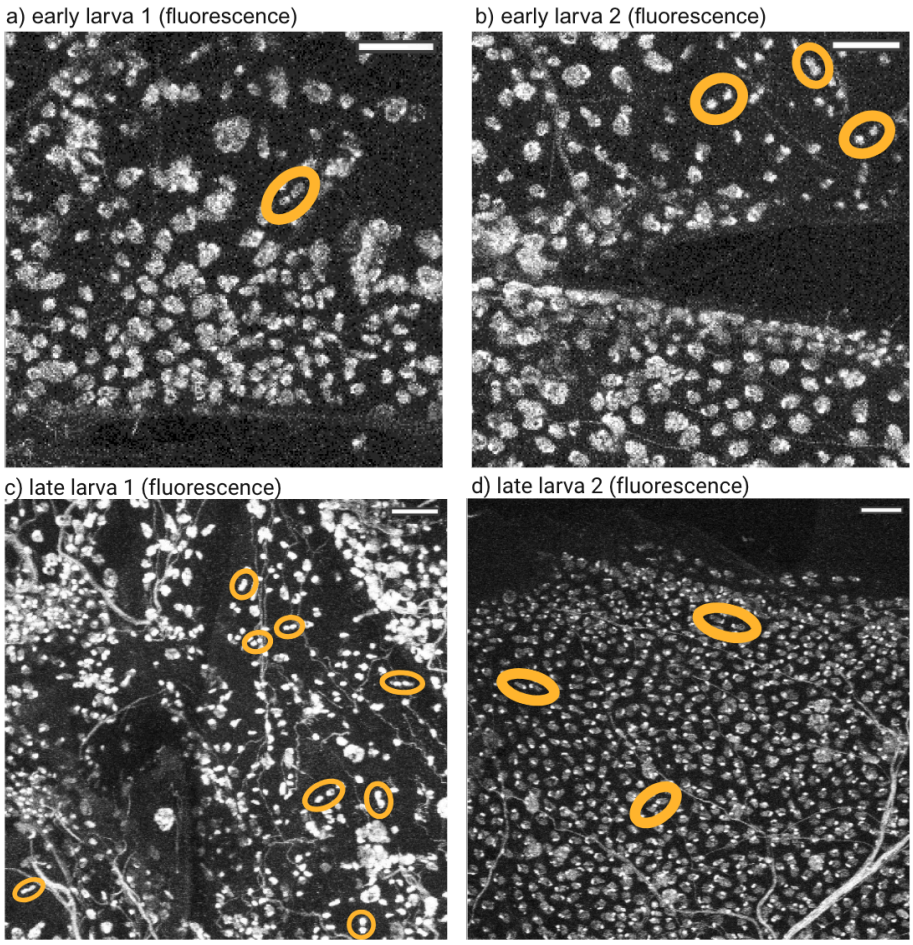

Fig. 12: Cell division in the abdomen of the early larval fourth instar (a-b) and late larval fourth instars (c-d) of *A. stephensi* (orange ellipse). All panels show a zoomed-in section of an abdominal segment where cell division was found to be occurring. Scale bars, 20 μm.

Pupal stages

Like the larval stages, the early and the late pupae also had a consistent nuclei distribution in the epithelium; however, the differences between the dorsal and ventral sides seen in the larvae were not observed for the pupae (Fig. 13). Moreover, there was no cell division recorded.

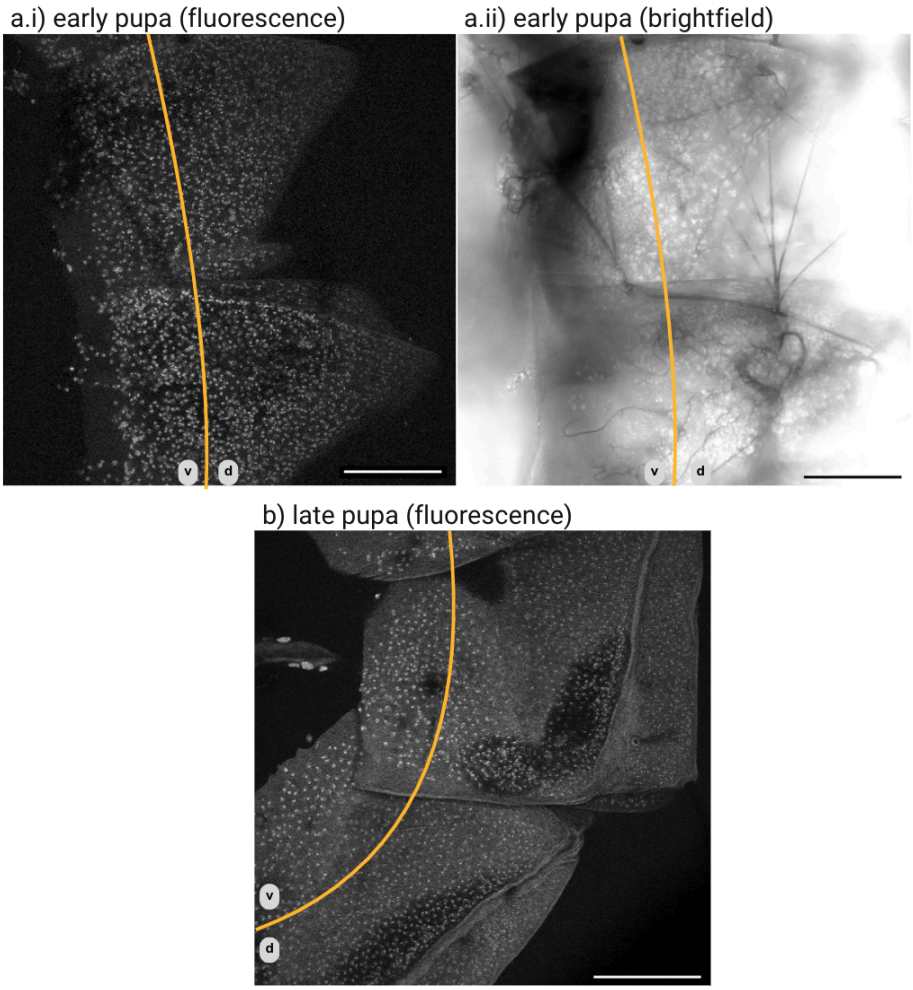

Fig. 13: The lateral perspective of the pupae abdomen of *A. stephensi*. The line across the abdominal segment shows the lateral axis dividing the dorsal (d) and ventral (v) sides. In panel a.i the nuclei diameter for the 20-minute old early pupa is 3.7 ± 0.7 µm, and in panel b the nuclei diameter for the 6-hour old late pupa is 4.4 ± 0.8 µm. The line down the middle of all the panels shows the lateral line dividing the dorsal (d) and ventral (v) sides, in addition to the segment indicator. Scale bars, 100 µm.

3.1.4 Decrease in nuclei diameter

The nuclei diameters visually appeared to decrease across the developmental stages (Tab. 1, Fig. 14). The early L4 had relatively larger epithelial cell nuclei compared to the subsequent stages, with the mean nuclei diameter being 6.0 ± 0.9 µm. The late L4 tended to exhibit an occasionally smaller cell nuclei diameter than the previous stage. Moreover, the early and the late pupae had nuclei diameters that were smaller. The early pupae had a mean nuclei diameter

of 5.2 ± 0.5 µm and the late pupae had a mean nuclei diameter of 4.9 ± 0.3 µm. The One-Way ANOVA test showed a significant difference for the nuclei diameters ($p<0.05$) of the developmental stages; however, Tukey's HSD post-hoc test demonstrated that there were no differences between the groups that could be considered statistically significant.

Tab. 1: Nuclei diameter measurements per developmental stage of *A. stephensi*

Stage	Average of 14 nuclei diameters (µm ± sd)					
	Sample 1	**Sample 2**	**Sample 3**	**Sample 4**	**Sample 5**	**Mean**
Early L4	6.5 ± 1.5	7.2 ± 1.6	6.1 ± 1.4	5.1 ± 0.9	5.2 ± 0.9	6.0 ± 0.9
Late L4	6.4 ± 0.9	6.7 ± 1.3	5.3 ± 0.7	6.3 ± 1.2	5.3 ± 0.7	6.0 ± 0.7
Early P	5.9 ± 1.0	4.8 ± 0.5	4.7 ± 0.9	5.3 ± 0.7	5.2 ± 0.9	5.2 ± 0.5
Late P	4.4 ± 1.0	4.9 ± 0.4	5.3 ± 0.6	5.0 ± 0.6	5.1 ± 0.6	4.9 ± 0.3

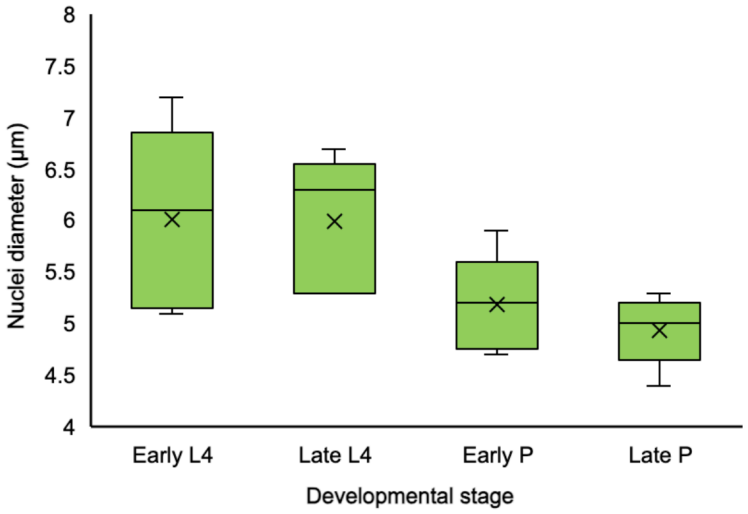

Fig. 14: Nuclei diameters in µm for the abdominal epithelia of *A. stephensi*. There appears to be a decrease in the nuclei diameters across the different developmental stages; however, Tukey's HSD showed there are no statistically significant differences between any of the stages.

3.1.5 Underneath the epithelium monolayer in *A. stephensi*

It was observed in over 18 images of the mosquito specimens (both larval and pupal) that underneath the epithelial monolayer there was a layer of cells with larger nuclei present (8.9 ± 1.8 µm diameter; n=5 images of early larvae, 5 images of late larvae, and 8 images of early pupae). These cells are likely fat body cells (Fig. 15; Chung *et al.*, 2017).

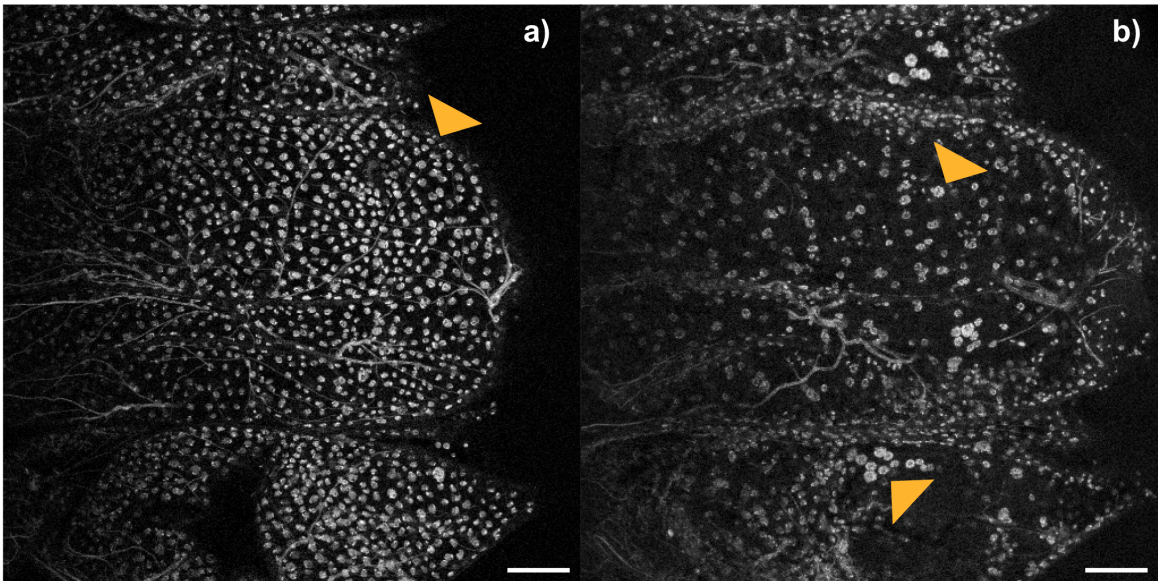

Fig. 15: The fat body cells present in the abdomen of *A. stephensi* 20-minute old early pupa. (a) shows the epithelial cells (nuclei diameter: 6.5 ± 1.6 µm) found at the surface (upper z-stacks). (b) shows the fat cell nuclei (nuclei diameter: 7.3 ± 1.4 µm) found underneath the epithelial layer in the lower z-stacks. Arrows point to the cells of interest. Scale bars, 50 µm.

3.2 Metamorphosis of the abdominal epidermis in a fungus gnat species

3.2.1 Appearance of epithelial nuclei in the abdomen

Larval stages

The fungus gnat abdominal epithelia of the larvae showed a pronounced difference to the mosquitoes. The epithelia of the early larvae were found to have cell populations with small nuclei on both the dorsal and ventral sides in between the larger LECs found in the centre of the abdomen (Fig. 16 and Fig. 17, Tab. 2).

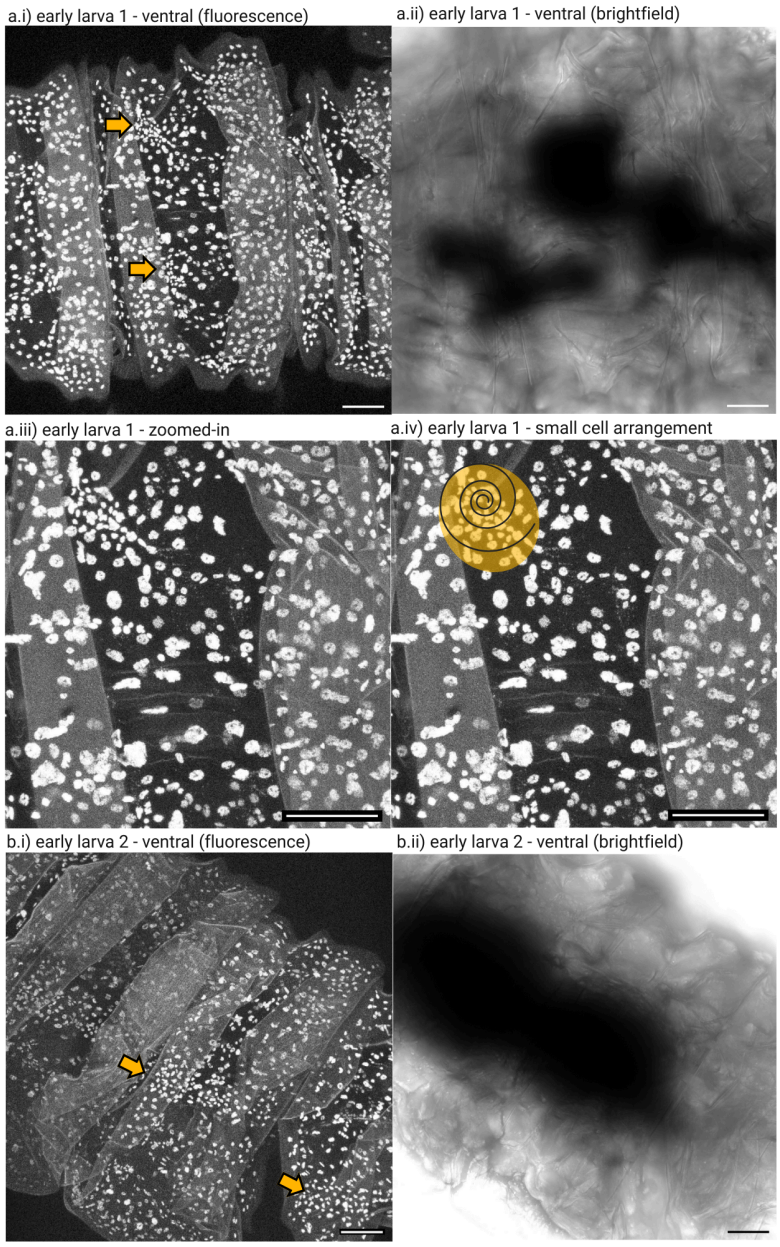

Fig. 16: Populations of cells with small nuclei can be found on the ventral side of the early larval fourth instar abdomens of the fungus gnat species. (a.i) Two small groups of cells with small nuclei are positioned in the anterior end of an abdominal segment. (a.ii) Transmitted light image of a.i). (a.iii) shows a zoom into the small cluster of cells in a.i) and (a.iv) illustrates the arrangement of the small cells that resembles a spiral pattern starting at the surface of the ventral epithelium and descending slightly deeper into the tissue. (b.i) Another example of a small population of cells with small nuclei positioned laterally; however, there are more nuclei than in (a.i), suggesting that the cells have undergone a few rounds of cell division in this larva.

The arrows point to areas with small nucleus cell populations. (a.i, a.iii, a.iv, b.i) are fluorescence images obtained using Hoechst staining, whilst (a.ii, b.ii) are transmitted light images. The transmitted light images were included to show that the ventral side was identified based on the absence of trachea. Scale bars, 50 μm.

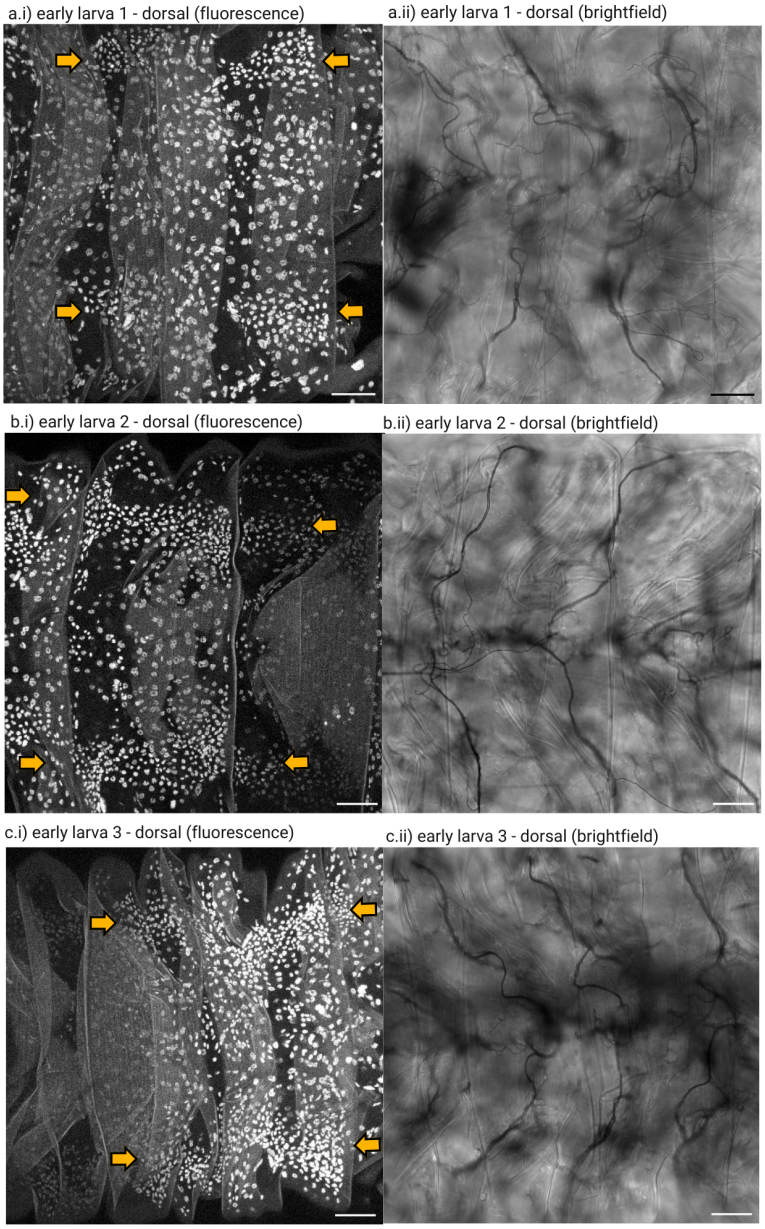

Fig. 17: Populations of cells with small nuclei can be found on the dorsal side of the early larval fourth instar abdomens of the fungus gnat species. (a.i) shows small nucleus cell populations clustered together on the lateral side of the abdomen that are distinct from the more widespread, larger LECs in the centre. It is hypothesized that the larvae in (b) and (c) are at a

slightly later stage due to the small nuclei cell populations in (b.i) and (c.i). There is an increase in the number of small nuclei cells from (a.i) to (b.i). (c.i) demonstrates a large increase in the lateral small cell populations compared to (a.i) and (b.i). The arrows point to areas with small cell populations. (a.i, b.i, c.i) are fluorescence images obtained using Hoechst staining, whilst (a.ii, b.ii, c.ii) are transmitted light images. The transmitted light images were included to show that the dorsal side can be identified using the tracheae that are connected to spiracles (Fig. 18). Scale bars, 50 µm.

Tab. 2: Averaged nuclei diameters of 14 cells in the abdominal epithelia of the fungus gnat species shown in Fig. 16 and Fig. 17.

Panel	Small nucleus cell diameter (µm ± sd)	Large nucleus cell diameter (µm ± sd)
Fig. 14a	2.9 ± 0.7	7.0 ± 1.0
Fig. 14b	3.0 ± 1.2	6.9 ± 0.8
Fig. 15a	4.0 ± 1.3	6.8 ± 1.6
Fig. 15b	3.9 ± 0.9	7.2 ± 1.1
Fig. 15c	4.2 ± 0.8	8.4 ± 1.4

On the ventral side of the early larval abdomen, the small nuclei (ca. 3.0 ± 0.9 µm diameter) were positioned in small nests that had around 25 cells (Fig. 16a.iii), which resemble histoblast nests in Drosophila (Roseland and Schneiderman, 1979; Madhavan and Madhavan, 1980). These small cell nests were found at the lateral-anterior end of the abdominal segment and were arranged in a circular pattern. The lower z-stacks revealed that these small nuclei descended slightly further into the tissue. The appearance of the ventral epithelial nuclei consistently showed widespread large LECs in the centre of the abdominal segment and smaller cell groups on the lateral side (Fig. 16). Fourteen images captured the epithelium on the ventral side, where 3 images captured the small cell nests on the ventral side seen in Fig. 16a.i and 4 showed the expanded small cells exemplified in 16b.i. The other seven images out of the fourteen showed wrinkled epithelia where it was difficult to interpret the cell composition. Nevertheless, the images (Fig. 16) had a marked visual difference in the small nuclei numbers, with Fig. 16b.i having more small nuclei. It is proposed that the larva in Fig. 16b.i is at a slightly later stage and that the small nuclei cells originated from the small cell clusters in (a.i) and have proliferated.

Unlike the ventral side, there were no circular small cell clusters on the dorsal side of the early larval abdomen. However, there were two larger lateral regions of cells with small nuclei (ca. 4.0 ± 1.4 µm diameter, Fig. 17a), with the LECs found around the dorsal midline. The three images of the dorsal side in Fig. 17, identified by the trachea (Fig. 17a.ii, 17b.ii, 17c.ii) connected to the lateral spiracles (Fig. 18), depicted the regions progressively increasing in size and nuclei density, possibly being an indicator of proliferation. Additionally, the z-stacks showed that these regions of small nuclei were only present in the uppermost layer of the epithelium.

In some instances, the Hoechst staining showed cell division of the cells with the small nuclei in the early larvae (Fig. 19). This shows that the hypothesized adult progenitor cells divide in the larva, unlike the histoblasts in *D. melanogaster* that do not divide in the larval stages and only undergo divisions in the pupal stage (Roseland and Scheiderman, 1979; Madhavan and Madhavan, 1980). The division of the small cells could help explain the decrease in the size of the cells as the organism undergoes metamorphosis and turns into a pupa (Fig. 19).

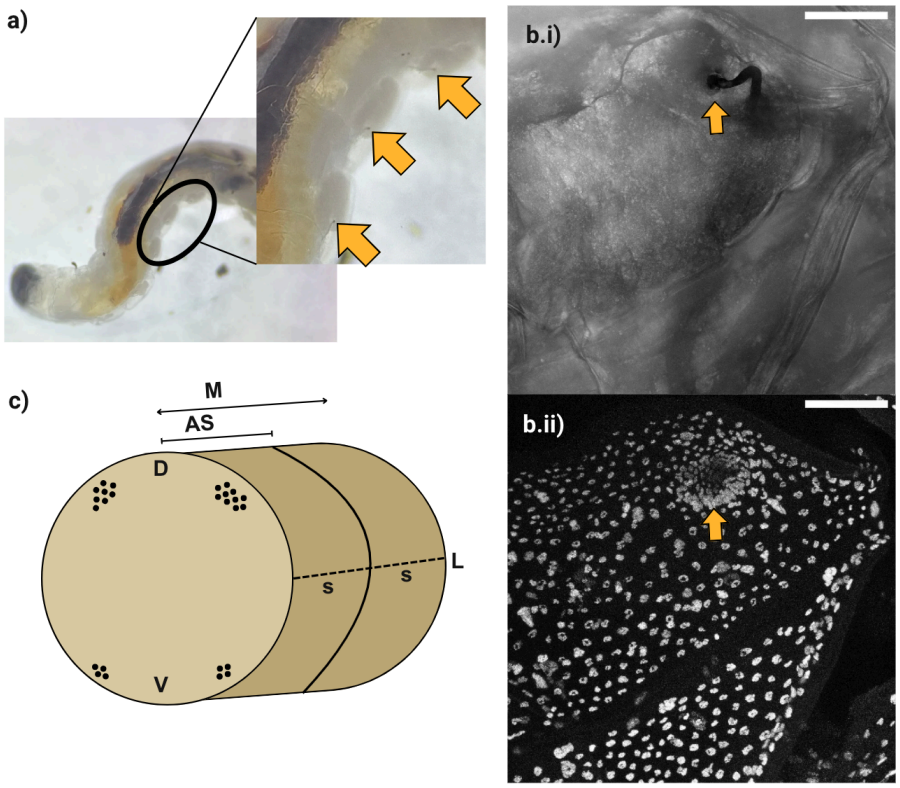

Fig. 18: The positioning of spiracle nests and the small cell populations in the epithelium of the early larval fourth instar of the fungus gnat species. (a) 3 small spiracles can be discerned on the lateral-dorsal side of an early L4. (b) shows a magnified lateral spiracle in the epithelium of an early larval fourth instar ((b.i) is transmitted light and (b.ii) is fluorescence). (c) Small nuclei

on the ventral (V) side were observed in smaller groups on either side of the midline (M) compared to the larger clusters on the dorsal (D) side. The dashed line on the side of the abdomen represents the lateral (L) side where spiracles (s) can be found on the abdominal segments (AS). Scale bars, 50 µm.

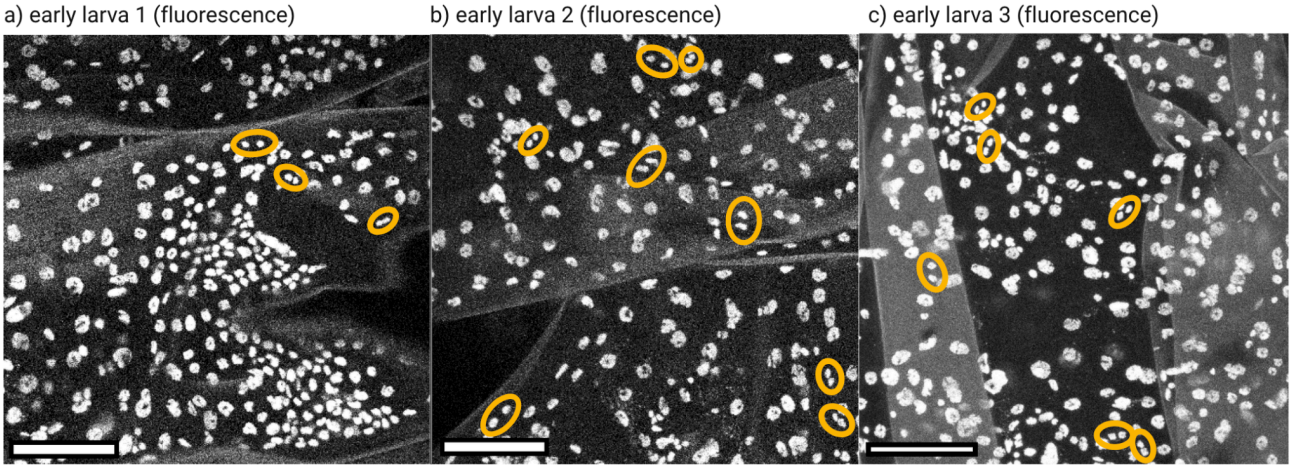

Fig. 19: Evidence for cell division in three early larval fourth instars of the fungus gnat species. (a) lateral side in early larva, (b,c) central areas of the abdominal segment. The nuclei diameters of the dividing cells are approximately 4.0 ± 0.6 µm. Scale bars, 50 µm.

Pupal stages

Compared to the larvae, the fungus gnat pupae have a much more homogeneous distribution of cells in the abdominal epithelia (Fig. 20), with no distinct small cell populations. The epithelial cells are visibly smaller compared to the larvae, and there was no cell division captured.

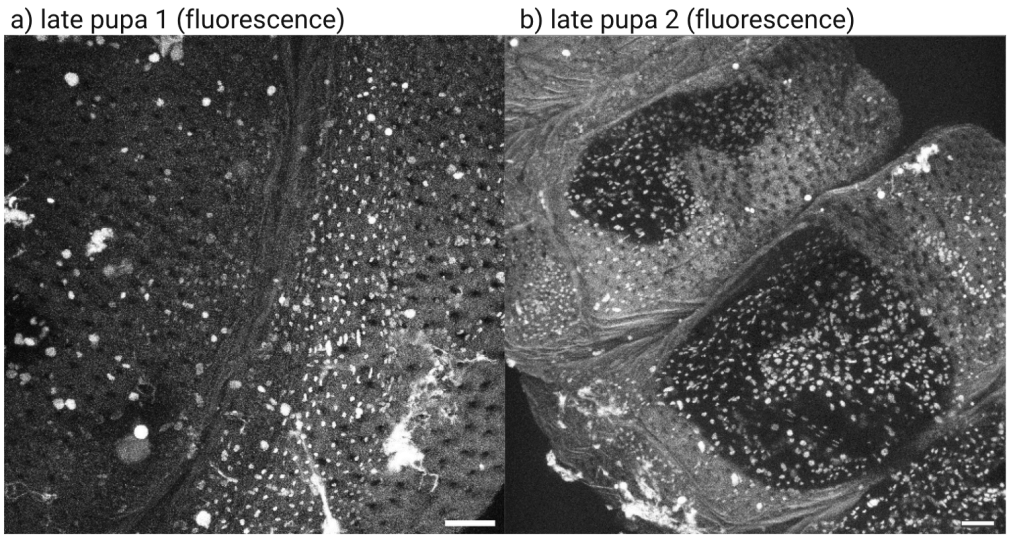

Fig. 20: Cells of the abdominal epithelium of the fungus gnat pupae. Nuclei diameters: 2.8 ± 0.3 µm (a), 3.9 ± 0.9 µm (b). Scale bars, 30 µm.

3.2.2 Decrease in nuclei diameters

The nuclei diameters decreased throughout development for the fungus gnats (Tab. 1, Fig. 21), with the nuclei diameter changing from 7.3 ± 0.3 µm in the early larva to 5.6 ± 0.6 µm in the late pupa. The One-Way ANOVA test revealed a significant difference for the nuclei diameters ($p<0.05$) of the developmental stages. Tukey's HSD post-hoc test further confirmed that there is a significant statistical difference between every developmental stage ($p<0.0001$).

Tab. 3: Nuclei diameter measurements per developmental stage of the fungus gnat

Stage	**Average of 14 nuclei diameters (µm ± sd)**						
	Sample 1	**Sample 2**	**Sample 3**	**Sample 4**	**Sample 5**	**Sample 6**	**Mean**
Early L4	7.1 ± 1.3	7.5 ± 1.6	7.9 ± 1.5	7.1 ± 1.7	7.0 ± 1.4	7.2 ± 0.9	7.3 ± 0.3
Late L4	6.0 ± 1.1	6.0 ± 0.8	6.2 ± 1.8	4.9 ± 0.8	5.5 ± 0.5	5.0 ± 0.5	5.6 ± 0.6
Late P	4.1 ± 1.3	3.6 ± 1.1	3.9 ± 0.6	4.4 ± 1.0	4.1 ± 1.1	3.9 ± 0.9	4.0 ± 0.3

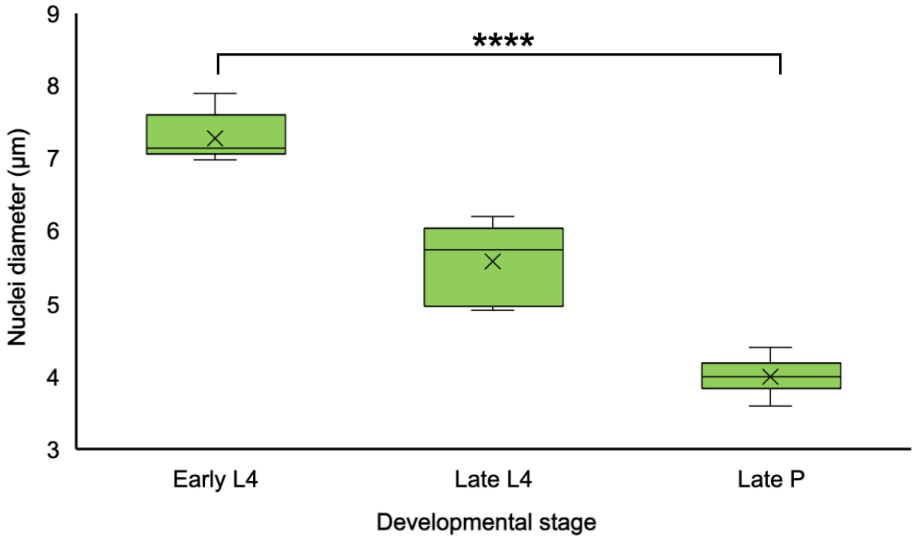

Fig. 21: Nuclei diameters in µm for the abdominal epithelia of fungus gnats. There is decrease in the nuclei diameters across the different developmental stages (early larval fourth instar (Early L4), late larval fourth instar (Late L4), late pupae (Late P)). Statistical significance, **** = p<0.0001.

4. Discussion

4.1 *A. stephensi*

My analysis of the adult abdominal epidermis of *A. stephensi* showed that its metamorphosis differs from that seen in *D. melanogaster*. In the *D. melanogaster* larvae, there are two distinguishable cell populations present in the single cell layer of the epithelium: the large polyploid LECs and the visibly smaller diploid histoblasts that afterwards proliferate across the abdominal segment from the lateral nests (Roseland and Schneiderman, 1979; Madhavan and Madhavan, 1980). There was no evidence to support the presence of imaginal progenitor cells in *A. stephensi*, with its epithelium demonstrating a visible homogenous monolayer beneath the cuticle (Fig. 10).

Underneath the epithelium, there were large nuclei that are hypothesized to be fat body cells due to their abundance (Fig. 15). Fat bodies were found in the abdomens of the *Aedes aegypti* mosquito; therefore, it can be proposed that the big cells in Fig. 15 are also fat cells. The large presence of these fat cells supports the abdomen being an energy storage site (Chung *et al.*, 2017). Chung *et al.* report that the fat bodies are organised in a sheaf-like manner linked to

the periphery of the abdominal cavity and that the cells composing the fat bodies, trophocytes, are large and polyploid. In essence, the fat bodies serve as an energy and nutrient source during abdominal metamorphosis (Arrese and Soulages, 2011).

The metamorphosis of the *A. stephensi* epithelium was characterized by cell division that occurred in the fourth larval instars (Fig. 12 and Tab. 1). Risler has already described in detail the mitotic events that affect the cell size over the course of development in *A. aegypti*. Upon reaching the fourth instar, the imaginal primordium in the epithelium undergoes several consequent mitoses, causing the cells to become tetraploid and increase in size as well as number (Risler, 1959). Then, directly before pupation when the fourth larval instar reaches and completes the fourth mitotic period, the nuclei diameter again decreases due to the somatic reduction of genetic material and the cell's return to the diploid state. This observation at a cellular level supports the mechanical aspect of the transition from a larva to pupa, where the larva's abdomen contracts and lengthens to form the pupa's abdomen that is smaller but has the same nuclei appearance (Risler, 1959). However, although it was not found in this report that mitosis events occur again a few hours post-pupation, it is possible that the timeframe was missed. Risler concludes by stating that whilst the proliferation and growth of nuclei assist in the growth of the larval epidermis, the nuclei in the pupa's epidermis, after a series of mitoses, eventually experience somatic reduction.

4.2 Fungus gnats

In the unidentified fungus gnat species, metamorphosis showed a greater resemblance to *D. melanogaster* metamorphosis. This is because in the fungus gnat ventral epithelium, I found cell populations distinct from the other epithelial cells that could be precursor cells on the lateral sides of the abdomen (Fig. 16 and Fig. 17). These cells seemed to proliferate (Fig. 17) and divide (Fig. 18), helping explain the decrease in nuclei diameter across the stages (Tab. 3).

The presented evidence for possible adult progenitor cells in fungus gnats (Fig. 14 and Fig. 16) provides a foundation for the hypothesis that pupal-stage cell replacement evolved within the Neodiptera. The absence of evidence of progenitor cells in *A. stephensi* found in this report, and the well-established observation of consistent cuticle-secreting polyploid epithelial cells in mosquitoes throughout development (Zhu *et al*., 2022) indicates that the mechanism of epidermal cell replacement driven by histoblast nests is a more derived condition present in later families (Truman, 2019). Concrete examples of the histoblast metamorphosis mode have

been reported for the later families, such as the Sepsidae, Calliphoridae, Sarcophagidae, Muscidae, and Drosophilidae (Bowsher and Nijhout, 2007; Madhavan and Madhavan, 1980; Madhavan and Madhavan, 1990; Melicher *et al.*, 2018; Pearson, 1977; Smith and French, 1991). However, there has been no documentation of histoblasts in earlier-diverging Neodipteran lineages. In contrast, it has been extensively documented that histoblasts are present in the Brachyceran branch (Madhavan and Madhavan, 1980; Ninov *et al.*, 2007; Bischoff and Cseresnyés, 2009). Therefore, if further experiments confirmed that histoblasts are indeed present in the Bibionomorpha, it would be the earliest lineage reported (with the others already aforementioned) to have precursor cells and would give an insight into the origins of this metamorphosis mode.

4.3 Morphology and mobility of both species' pupae

The observed differences in abdominal metamorphosis may reflect the differences in the level of predation which fungus gnats and mosquitoes encounter during metamorphosis. Like *D. melanogaster* pupae (White *et al*., 2022), the soil-inhabiting fungus gnat pupae are immobile, which could be explained by an environment where active predator avoidance is not advantageous (Lindstedt *et al*., 2019). On the other hand, the aquatic mosquito pupae are highly mobile and found in ponds, which have a high predation pressure. The mobility is due to the long abdomen, which allows the mosquito pupae to quickly swim away. I hypothesise that this mobility can only be maintained during the pupal stage when the abdominal epidermis is not remodelling, but quickly reprogramming.

4.4 Considerations

A factor that could have influenced the results of this study that was not accounted for is the sex of the specimens selected for dissections. This would be possible as Emami *et al.* have described the possibility of determining the sex as early as the late third larval instar (Emami *et al.*, 2007). Moreover, the abdominal segments used for imaging were not identical. Therefore, potential regional differences between the segments could affect the conclusions made.

5. Outlook

Fully characterizing metamorphosis in the Nematocerans is a large undertaking that could not be accomplished with the timeframe and the materials used in this investigation. More detailed analyses of a larger number of stages would be necessary. To determine whether the observed small cell populations in the fungus gnat are indeed adult progenitor cells, it would be necessary to attempt to localize the Escargot (Esg) protein in these cells (e.g. by using the Drosophila antibody if it cross-reacts in fungus gnats). Esg has been shown in Drosophila to maintain the diploid state of adult progenitor cells (Fuse *et al.*, 1994). Staining Esg would help clarify whether it is larval or adult cells that are dividing in the fungus gnats. To place these observations into the context of cellular events, it would be necessary to perform fluorescence *in situ* hybridization to be able to look at ploidy and chromosome numbers during mitosis of the organisms (Timoshevskiy, 2012). *In vivo* imaging would be another experimental technique that would shed light on the potential cell replacement mechanism in the fungus gnats. However, this would require establishing live imaging protocols and culturing fungus gnat flies that express a fluorescent marker (e.g. histone-GFP; Sakai *et al.*, 2009) to visualize the remodelling of the abdominal epithelia. Additionally, it would be advisable to repeat the fungus gnat study in a well-characterised laboratory strain (e.g. Bradysia coprophila (Gerbi, 2024)). Finally, it would be interesting to expand the scope of this study by examining more lower fly genera, such as Chaoboridae (one of the most recent lineages of Culicomorpha; Wiegmann *et al*., 2011) and Anisopodidae (the earliest lineage of Bibionomorpha; Henrique, 2023), allowing for the determination of when cell replacement-based metamorphosis appeared in the Diptera (Fig. 2; Truman, 2019).

Acknowledgements

I am very grateful for having had the chance to pursue research linked to developmental biology, a field I was always curious about. I would like to thank Lord Laidlaw for making this opportunity possible through the Laidlaw Foundation. Additionally, I want to express my gratitude to my supervisor, Dr. Marcus Bischoff, for providing expert guidance and support throughout the project and the revision of the report. Lastly, I would like to acknowledge and thank Sarah Reece, Ronnie Mooney, and Aidan O'Donnell from the University of Edinburgh for providing the *A. stephensi* mosquito larvae.

References

Arrese, E.L. and Soulages, J.L. (2010). Insect Fat Body: Energy, Metabolism, and Regulation. *Annual Review of Entomology*, [online] 55(1), pp.207–225. doi:https://doi.org/10.1146/annurev-ento-112408-085356.

Bowsher, J.H. and Nijhout, H.F. (2007). Evolution of novel abdominal appendages in a sepsid fly from histoblasts, not imaginal discs. *Evolution & Development*, [online] 9(4), pp.347–354. doi:https://doi.org/10.1111/j.1525-142x.2007.00171.x.

Chung, H.-N., Rodriguez, S.D., Carpenter, V.K., Vulcan, J., Bailey, C.D., Madhugiri Nageswara-Rao, Li, Y., Attardo, G.M. and Hansen, I.A. (2017). Fat body organ culture system in *Aedes Aegypti*, a vector of Zika virus. *Journal of Visualized Experiments*, [online] (126). doi:https://doi.org/10.3791/55508.

Emami, S.N., Vatandoost, H., Oshaghi, M.A., Mohtarami, F., Javadian, E. and Raeisi, A. (2007). Morphological method for sexing Anopheline larvae. *Journal of Vector Borne Diseases*, [online] 44(4), pp.245–249. Available at: https://pubmed.ncbi.nlm.nih.gov/18092530/. (Accessed: 29 August 2025).

Fuse, N., Hirose, S. and Hayashi, S. (1994). Diploidy of Drosophila imaginal cells is maintained by a transcriptional repressor encoded by escargot. *Genes Dev.*, [online] 8(19), pp.2270–2281. doi:https://doi.org/10.1101/gad.8.19.2270.

Gerbi, S.A. (2024). Laboratory maintenance of the lower Dipteran fly *Bradysia* (Sciara) *coprophila*: A new/old emerging model organism. *Journal of Visualized Experiments*, [online] (206). doi:https://doi.org/10.3791/66751.

Gillespie, D.R. (1986). A simple rearing method for fungus gnats *Corynoptera sp.* (Diptera: Sciaridae) with notes on life history. *Journal of the Entomological Society of British Columbia*, [online] 83. Available at: https://journal.entsocbc.ca/index.php/journal/article/view/2225. (Accessed: 29 August 2025).

Kassambara, A. (2023). rstatix: Pipe-friendly framework for basic statistical tests. *R package version 0.7.2*. Available at: https://CRAN.R-project.org/package=rstatix. (Accessed: 29 August 2025).

Kuiter, R.H. (2020). Pollination by sexual deception of different fungus-gnat species, two (Mycetophilidae) in *Pterostylis grandiflora* and two (Sciaridae) in *P. nana* (Orchidaceae). *The Victorian Naturalist*, [online] 137(2-2020), pp.41-47. Available at: https://www.researchgate.net/publication/341667087_Pollination_by_sexual_deception_of_different_fungus-gnat_species_two_Mycetophilidae_in_Pterostylis_grandiflora_and_two_Sciaridae_in_P_nana_Orchidaceae. (Accessed: 29 August 2025).

Kumaran, A.K. (1978). Reprogramming and DNA synthesis in *Galleria mellonella* larval epidermal cells. *Differentiation*, [online] 12(2), pp.121–125. doi:https://doi.org/10.1111/j.1432-0436.1979.tb00997.x.

Lindstedt, C., Murphy, L. and Mappes, J. (2019). Antipredator strategies of pupae: how to avoid predation in an immobile life stage? *Philosophical Transactions of the Royal Society B: Biological Sciences*, [online] 374(1783), pp.1-11. doi:https://doi.org/10.1098/rstb.2019.0069.

Madhavan, M.M. and Madhavan, K. (1980). Morphogenesis of the epidermis of the adult abdomen of Drosophila. *Development*, [online] 60(1), pp.1–31. doi:https://doi.org/10.1242/dev.60.1.1.

Madhavan, K. and Madhavan, M.M. (1990). Pattern regulation in the ventral histoblasts of the housefly: induction of sternal pattern abnormalities by mechanical wounding of larval epidermal cells. *Developmental Biology*, [online] 139(1), pp.42–55. doi:https://doi.org/10.1016/0012-1606(90)90277-p.

Melicher, D., Su, K.F.Y., Meier, R. and Bowsher, J.H. (2018). Comparative analysis reveals the complex role of histoblast nest size in the evolution of novel insect abdominal appendages in Sepsidae (Diptera). *BMC Evolutionary Biology*, [online] 18(1). doi:https://doi.org/10.1186/s12862-018-1265-3.

Ninov, N., Chiarelli, D.A. and Martin-Blanco, E. (2007). Extrinsic and intrinsic mechanisms directing epithelial cell sheet replacement during Drosophila metamorphosis. *Development*, [online] 134(2), pp.367–379. doi:https://doi.org/10.1242/dev.02728.

Nishiura, J.T. (2002). Coordinated morphological changes in midgut, imaginal discs, and respiratory trumpets during metamorphosis of *Aedes aegypti* (Diptera: Culicidae). *Annals of the Entomological Society of America*, [online] 95(4), pp.498–504. doi:https://doi.org/10.1603/0013-8746(2002)095[0498:cmcimi]2.0.co;2.

Pearson, M.J. (1977). Pattern and polarity of sclerites in adult abdominal segments of Calliphora erythrocephala (Diptera): anlage rotation experiments. *Journal of Embryology and Experimental Morphology*, [online] 37(1), pp.91–104. Available at: https://pubmed.ncbi.nlm.nih.gov/870595/. (Accessed: 29 August 2025).

R Core Team (2024). R: A Language and Environment for Statistical Computing. *R Foundation for Statistical Computing*. Available at: https://www.R-project.org/. (Accessed: 29 August 2025).

Risler, H. (1959). Polyploidie und somatische reduktion in der larvenepidermis von *Aedes aegypti L.* (Culicidae). *Chromosoma*, [online] 10(1-6), pp.184–209. doi:https://doi.org/10.1007/bf00396571.

Roseland, C.R. and Schneiderman, H.A. (1979). Regulation and metamorphosis of the abdominal histoblasts of *Drosophila Melanogaster*. *Wilhelm Roux Archives of Developmental Biology*, [online] 186(3), pp.235–265. doi:https://doi.org/10.1007/bf00848591.

Sakai, A., Schwartz, B.S., Goldstein, S. and Ahmad, K. (2009). Transcriptional and developmental functions of the h3.3 histone variant in Drosophila. *Current Biology*, [online] 19(21), pp.1816–1820. doi:https://doi.org/10.1016/j.cub.2009.09.021.

Schindelin, J., Arganda-Carreras, I., Frise, E., Kaynig, V., Longair, M., Pietzsch, T., Preibisch, S., Rueden, C., Saalfeld, S., Schmid, B., Tinevez, J.-Y., White, D.J., Hartenstein, V., Eliceiri, K., Tomancak, P. and Cardona, A. (2012). Fiji: an open-source platform for biological-image analysis. Nature Methods, 9(7), pp.676–82. doi:https://doi.org/10.1038/nmeth.2019.

Sedlak, B.J. and Gilbert, L.I. (1976). Epidermal Cell development during the pupal-adult metamorphosis of Hyalophora cecropia. *Tissue & cell*, [online] 8(4), pp.637–648. doi:https://doi.org/10.1016/0040-8166(76)90036-7.

Smith, H. and French, V. (1991). Pattern regulation during the development of the dorsal abdomen in the flesh fly, *Sarcophaga agryostoma*. *Roux's Archives of Developmental Biology*, [online] 200(5), pp.256–268. doi:https://doi.org/10.1007/bf00241295.

Timoshevskiy, V.A., Sharma, A., Sharakhov, I.V. and Sharakhova, M.V. (2012). Fluorescent in situ hybridization on mitotic chromosomes of mosquitoes. *Journal of Visualized Experiments*, [online] (67). doi:https://doi.org/10.3791/4215.

Truman, J.W. (2019). The evolution of insect metamorphosis. *Current Biology*, [online] 29(23), pp.1252–1268. doi:https://doi.org/10.1016/j.cub.2019.10.009.

Truman, J.W. and Riddiford, L.M. (1999). The origins of insect metamorphosis. *Nature*, 401(6752), pp.447–452. doi:https://doi.org/10.1038/46737.

White, J.S., LaFever, K.S. and Page-McCaw, A. (2022). Dissecting, fixing, and visualizing the Drosophila pupal notum. *Journal of Visualized Experiments*, [online] (182). doi:https://doi.org/10.3791/63682.

Wiegmann, B.M., Trautwein, M.D., Winkler, I.S., Barr, N.B., Kim, J.-W. ., Lambkin, C., Bertone, M.A., Cassel, B.K., Bayless, K.M., Heimberg, A.M., Wheeler, B.M., Peterson, K.J., Pape, T., Sinclair, B.J., Skevington, J.H., Blagoderov, V., Caravas, J., Kutty, S.N., Schmidt-Ott, U. and Kampmeier, G.E. (2011). Episodic radiations in the fly tree of life. *Proceedings of the National Academy of Sciences*, [online] 108(14), pp.5690–5695. doi:https://doi.org/10.1073/pnas.1012675108.

Zhu, G.H., Gaddelapati, S.C., Jiao, Y., Koo, J. and Palli, S.R. (2022). CRISPR-Cas9 genome editing uncovers the mode of action of methoprene in the yellow fever mosquito, *Aedes aegypt*i. *The CRISPR Journal*, [online] 5(6), pp.813–824. doi:https://doi.org/10.1089/crispr.2022.0066.